Nuclear Engineering and Design 337 (2018) 378–393

Contents lists available at ScienceDirect

Nuclear Engineering and Design

journal homepage: www.elsevier.com/locate/nucengdes

Characterization of salt deposit layer growth and prediction of cladding temperature of heated rod bundles under long-term seawater injection and pool boiling conditions

Miyuki Akiba*, Akitoshi Hotta, Retsu Kojo

Regulatory Standard and Research Department, Secretariat of Nuclear Regulation Authority, 1-9-9, Roppoingi, Minato-ku, Tokyo 106-8450, Japan

ARTICLE INFO

Keywords:
Severe accident
Seasalt
Precipitation
Deposit
X-Ray computer tomography
Heat removal

ABSTRACT

Seawater has been recognized as an alternative water source in severe accident countermeasures even before the TEPCO Fukushima Dai-ichi NPS accident. In this article, influences of deposit layers of salt precipitates on the early core degradation were investigated. A heated part of a fuel bundle was regarded as a major deposit site and numerical models for predicting growing geometry of deposit layers and resultant temperature responses of cladding were developed. These models have been validated based on precipitation tests employing 5×5 short length mockup bundles submerged in solutions of simple seawater and a mixture of seawater and boric acid.

Growth and geometry of salt deposit layers were expressed as a product of the shape function and Matsuoka's kinetic law (Matsuoka, 1991) where the growth factor is expressed by the Arrhenius law. Model parameters of the kinetic law and the shape function were quantified based on digitized image data of deposit layers acquired in the abovementioned precipitation tests based on the X-Ray CT scan. Combining with the axial onedimensional two-phase flow model, the effective heat transfer coefficient of the cladding surface was evaluated taking into account growth of deposit layers and two-phase flow regimes. Finally, cladding temperature responses were evaluated based on the energy balance. Final geometry of salt deposit layers was digitized under a wide range of pool boiling conditions based on image data acquired in precipitation tests employing 5×5 short length mockup bundles. Based on these data, the shape function of each test case was reduced. It was confirmed that Matsuoka's kinetic law could predict a total mass increase of deposit layers with a good accuracy by specifying a constant in the Arrhenius law as nearly equivalent values for all test cases. From a comparison of measured and predicted surface temperatures at the exit of a heated length of the center rod, it can be interpreted that temperature increased gradually after the salt concentration reached the saturation point, then temperature began to increase steeply when a gap formed by neighboring rods was closed and isolated chimney flow paths surrounding the center heater rod were formed. Another important finding is that there was a certain margin of time until chimneys were formed after reaching the saturated salt concentration, which indicates feasibility of a practical fast running evaluation model based on decay heat, average salt concentration and boundary conditions that can be estimated to a certain degree of confidence level even under accident conditions.

1. Introduction

In the TEPCO Fukushima Daiichi NPS accident caused by the Great East Japan Earthquake and subsequent tsunamis on March 11th 2011, the entire plant site was placed under harsh conditions caused by station blackout and loss of ultimate heat sinks occurring in multiple plants simultaneously. Seawater was directly injected into the core for more than one week (TEPCO, 2012). In severe accident management guidelines of pressurized water reactors (PWRs) and boiling water reactors (BWRs) applied for operation under the new safety regulation, seawater has been recognized as an alternative water source that can be injected into the reactor, the secondary side of steam generators and the spent fuel pool.

Under long term seawater injection, coolant boils up due to high decay heat and the salt concentration increases gradually. If the concentration exceeds locally the saturation point (estimated to be about 28.15% for sodium chloride in present studies) in flow stagnant region, salt precipitates appear in coolant. Then these precipitates will be flown in coolant and will be agglomerated on surfaces of fuel bundles, the lower plenum and elsewhere in the reactor pressure vessel and deposit

* Corresponding author.
E-mail address: miyuki_akiba@nsr.go.jp (M. Akiba).

https://doi.org/10.1016/j.nucengdes.2018.07.012
Received 1 October 2017; Received in revised form 9 July 2018; Accepted 10 July 2018

Nomenclature

Latin

A	frequency factor of reaction in the Arrhenius law (kg/sec)
B	activation energy of reaction in the Arrhenius law (J/mol)
c	salt concentration (kg/kg)
c_{sat}	saturated concentration of salt (kg/kg)
C_p	cladding heat capacity at constant pressure (J/kg/K)
d	arbitrary exponent in the Arrhenius law (−)
D_e	hydraulic equivalent diameter (m)
f	friction loss coefficient (−)
F_{in}	energy supply into cladding (W/m^3)
F_{out}	energy removal from cladding (W/m^3)
g	gravity acceleration (m/sec^2)
G	mass flux (kg/m^2/sec)
H_{D-B}	Dittus-Boelter's single phase forced convection heat transfer coefficient (W/m^2/K)
H_f	combined two-phase flow heat transfer coefficient (W/m^2/K)
H_K	Kutateladze's nucleated boiling heat transfer coefficient (W/m^2/K)
h_{gl}	latent heat of water evaporation (J/kg)
j	superficial velocity (m/sec)
k_r	precipitation growth factor (kg/sec)
K_{spacer}	spacer local loss coefficient (−)
l_a	Laplace length $\{\sigma/g(\rho_l-\rho_g)\}^{1/2}$ (m)
P	system pressure (Pa)
Pr	Prandtl number (−)
q	heat flux (W/m^2)
Q	heat generated from heater rod surfaces (W)
R	universal gas constant (J/K/mol)
S	lumped or distributed mass of salt deposit layers (kg)
T	water temperature (K)
T_w	cladding average temperature (K)
w_p	incremental mass of precipitates (kg)

Greek

α	void fraction
ΔV	evaporated volume (m^3)
δ	deposit layer thickness (m)
δc	degree of supersaturation of salt concentration ($(c-c_{sat})/c_{sat}$) (−)
ε	porosity of deposit layer (−)
θ	location index of the azimuthal section around each heater rod (−)
ρ	density (kg/m^3)
λ	thermal conductivity (W/m/K)
μ	viscosity (Pa·s)
ν	dynamic viscosity (m^2/sec)
σ	surface tension (N/m)
Φ_{l0}^2	two phase multiplier of friction loss (−)
χ	vapor quality (−)

Subscript indexes

c	cladding
g	vapor phase
i	row index of heater rods in bundle (−)
j	column index of heater rods in bundle (−)
k	axial index of heater rods in bundle (−)
l	liquid phase
m	mixture of liquid and vapor
s	seasalt
0	initial state when heating is started

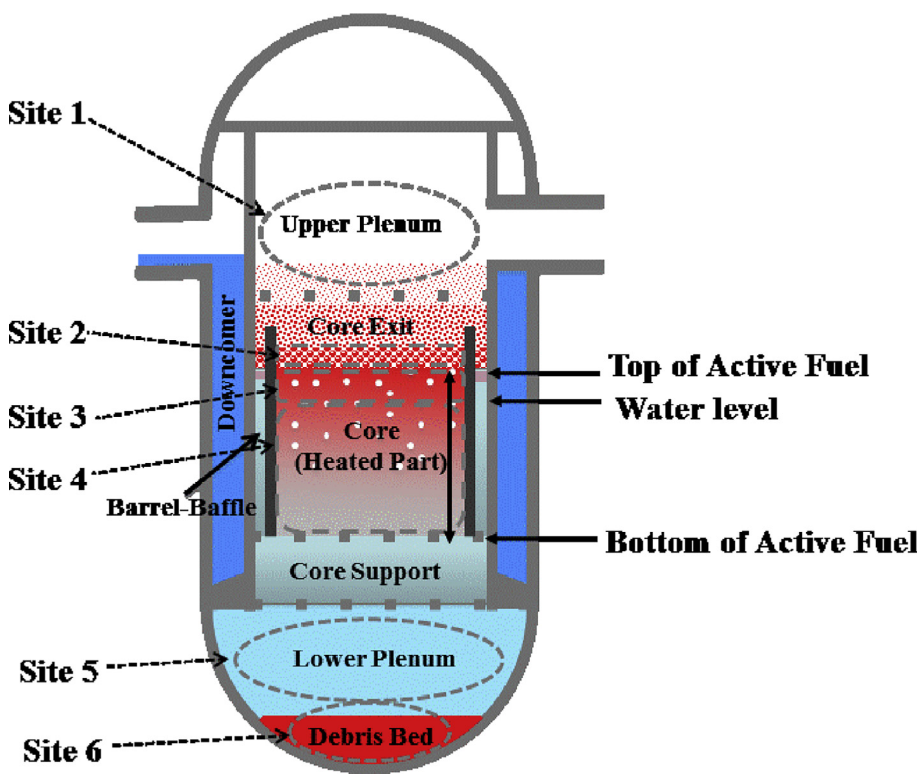

Fig. 1. Six potential sites of deposit layers of salt precipitates under seawater injection.